



Terminal pyridine-N ligation at [FeFe] hydrogenase active-site mimic

Yue Zhang, Ming-Qiang Hu, Hui-Min Wen, You-Tao Si, Cheng-Bing Ma, Chang-Neng Chen*, Qiu-Tian Liu

Fujian Institute of Research on the Structure of Matter, No. 155 West Yangqiao Road, Chinese Academy of Sciences, Fuzhou, Fujian 350002, PR China

ARTICLE INFO

Article history:

Received 23 February 2009

Received in revised form 30 March 2009

Accepted 31 March 2009

Available online 14 April 2009

Keywords:

Bioinorganic chemistry

Electrochemistry

[FeFe] Hydrogenase

Organometallic complexes

Pyridine ligand

ABSTRACT

Diiron model complexes $(\mu\text{-pdt})\text{Fe}_2(\text{CO})_5\text{L}$ with L = pyridine ligands, e.g. py (**A**), etpy (**B**), btpy (**C**), were synthesized as active site analogues of [FeFe] hydrogenase, and characterized by X-ray crystallography and electrochemistry. Pyridine-N ligation was found to be able to tune the redox properties of the diiron centers of model complexes.

© 2009 Elsevier B.V. All rights reserved.

1. Introduction

[FeFe] hydrogenase has sparked chemical mimic research interest due to the capability of producing hydrogen efficiently. The active site has been called “H-cluster”, which comprises a dithiolate-bridged diiron subsite and a cuboidal $\text{Fe}_4\text{S}_4(\text{S-Cys})_4$ cluster, linked up through a cysteine sulfur atom. Chemical model studies have shown that classical Reihlen diiron dithiolate complexes $(\mu\text{-SR})_2\text{Fe}_2(\text{CO})_6$ share several structural features with the diiron subsite, e.g. short Fe–Fe distance (ca. 2.6 Å), bidentated dithiolate bridge and diatomic CO ligands [1–3].

To obtain better structural and functional diiron model complexes, good donor ligands, such as carbene [4–7], cyanide [8–12], phosphine [13–18], thioether or sulfoxide [19,20], have been introduced into diiron model complexes by the method of CO-displacement of $(\mu\text{-pdt})\text{Fe}_2(\text{CO})_6$ (**1**). While the structural models of the active site of [FeFe] Hydrogenase have matured considerably over recent years [21–25], little attention has been devoted to the influence of the N-ligation at diiron models, for it is difficult to isolate the labile coordination of the amine to iron atom, for instance in $(\mu\text{-pdt})\text{Fe}_2(\text{CO})_5(\text{NH}_2\text{Pr})$ (**2**) which is unstable [26].

But the electron-donating capability of the nitrogen atom is expected in N-ligation of nitrogen-heterocycles, which are abundant in nature and play important role in organometallic chemistry. We thought it would be interesting to evaluate the role of N-ligation in diiron model complexes with the introduction of pyridine or other heterocyclic-N ligands [27], which was expected to extend new promising models for structural or functional modification

for 2Fe2S model complexes. Herein, we report the preparation of a series of active site analogues of [FeFe] hydrogenase with the substitution of pyridine ligands, and their characterization and electrochemistry.

2. Experimental

2.1. Reagents and measurements

All manipulations and reactions were carried out under dry oxygen-free N_2 using standard Schlenk techniques. All chemicals were analytical reagents and used without further purification. The compounds etpy, btpy (Supplementary) and $(\mu\text{-pdt})\text{Fe}_2(\text{CO})_6$ (**1**) [28,29] were prepared according to the literature. All solvents were dried and distilled prior to use according to the standard methods. Infrared spectra were recorded on a Perkin–Elmer Spectrum One FT-IR spectrophotometer using KBr pellets. ^1H NMR spectra were collected on a Varian Unity 500NMR spectrometer. Mass spectra were recorded on a DECAX-3000 LCQ Deca XP instrument. Elemental analysis was carried out on a Vario EL III Elemental Analyser.

2.2. Preparations

2.2.1. Preparation of $(\mu\text{-pdt})\text{Fe}_2(\text{CO})_5\text{Py}$ (**A**)

$(\mu\text{-pdt})\text{Fe}_2(\text{CO})_6$ (3 mmol, 1.158 g) (**1**) reacted with $\text{Me}_3\text{NO} \cdot 2\text{H}_2\text{O}$ (3 mmol, 0.333 g) under the ice bath condition in 30 mL of CH_3CN , and then pyridine (3 mmol, 0.237 g) was added. The colour turned from red into black. After 24 h the solvent was filtered and evaporated under vacuum. The remaining residue was extracted with 30 mL of freshly distilled *n*-hexane and filtered. Dark

* Corresponding author. Tel./fax: +86 591 8379 2395.
E-mail address: ccn@fjirsm.ac.cn (C.-N. Chen).

crystals were obtained after several days in the refrigerator at $-20\text{ }^{\circ}\text{C}$. Yield: 70% (0.92 g). Anal. Calcd for $\text{Fe}_2\text{S}_2\text{C}_{13}\text{O}_5\text{H}_{11}\text{N}$: C, 35.73; H, 2.54; N, 3.21. Found: C, 35.54; H, 2.59; N, 3.14%. IR (cm^{-1} , KBr pellet): (ν_{CO}) 2029 (s), 1980 (vs), 1939 (m), 1918 (m). ^1H NMR (CD_3CN): δ 8.36 (2H, Py), 7.33 (1H, Py), 7.20 (2H, Py), 2.15 (4H, $\text{SCH}_2\text{CH}_2\text{CH}_2\text{S}$), 1.85 (2H, $\text{SCH}_2\text{CH}_2\text{CH}_2\text{S}$). m/z 437.7 [$\text{M}+\text{H}$] $^+$.

2.2.2. Preparation of $(\mu\text{-pdt})\text{Fe}_2(\text{CO})_5(\text{etpy})$ (**B**)

The reaction steps were similar to those of **A**, but 4-(ethylthio)pyridine (3 mmol, 0.418 g) was used to replace pyridine. Yield: 60% (0.89 g). Anal. Calcd for $\text{Fe}_2\text{S}_3\text{C}_{15}\text{O}_5\text{H}_{15}\text{N}$: C, 36.24; H, 3.04; N, 2.82. Found: C, 37.19; H, 3.11; N, 2.97%. IR (cm^{-1} , KBr pellet): (ν_{CO}) 2033 (s), 1978 (vs), 1918 (m). ^1H NMR (CD_3CN): δ 8.36 (2H, Py), 7.19 (2H, Py), 2.16 (4H, $\text{SCH}_2\text{CH}_2\text{CH}_2\text{S}$), 2.13 (2H, SCH_2CH_3), 1.85 (2H, $\text{SCH}_2\text{CH}_2\text{CH}_2\text{S}$), 1.36 (3H, SCH_2CH_3). m/z : 498.7 [$\text{M}+\text{H}$] $^+$, 414.9 [$\text{M}+\text{H}-3\text{CO}$] $^+$.

2.2.3. Preparation of $[(\mu\text{-pdt})\text{Fe}_2(\text{CO})_5(\text{btpy})]$ (**C**)

The reaction steps were similar to those of **A**, but 4-(*n*-butylthio)pyridine (3 mmol, 0.501 g) was used to replace pyridine. Yield: 64% (1.01 g). Anal. Calcd for $\text{Fe}_2\text{S}_3\text{C}_{17}\text{H}_{19}\text{O}_5\text{N}$: C, 38.88; H, 3.65; N, 2.67. Found: C, 38.84; H, 3.78; N, 2.53%. IR (cm^{-1} , KBr pellet): (ν_{CO}) 2038 (s), 1969 (vs), 1953 (s), 1920 (m). ^1H NMR (CD_3CN): δ 8.37 (2H, Py), 7.21 (2H, Py), 2.46 (2H, $\text{SCH}_2\text{CH}_2\text{CH}_2\text{CH}_3$), 2.15 (4H, $\text{SCH}_2\text{CH}_2\text{CH}_2\text{S}$), 1.86 (2H, $\text{SCH}_2\text{CH}_2\text{CH}_2\text{S}$), 1.69 (2H, $\text{SCH}_2\text{CH}_2\text{CH}_2\text{CH}_3$), 1.35 (2H, CH_2CH_3), 0.95 (3H, CH_2CH_3). m/z : 525.9 [$\text{M}+\text{H}$] $^+$.

2.3. X-ray crystallography

Diffraction measurements of single crystals of complexes **A** and **B** were made on a Rigaku Mercury diffractometer using graphite

monochromated Mo $\text{K}\alpha$ radiation ($\lambda = 0.71073\text{ \AA}$), while single crystal of complex **C** was performed on a Rigaku Saturn70 diffractometer. Crystal data collection, refinement and reduction were accomplished with the CRYSTALCLEAR processing program. The structure was solved by direct methods with SHELXS-97 [30] and refined by using the SHELXL-97 crystallographic software package [31]. All non-hydrogen atoms were refined anisotropically. The hydrogen atoms were added in a riding model, while the pdt bridge in **C** was refined with “envelope-flap” disorder. Crystallographic data of **A**, **B** and **C** are summarized in Table 1.

2.4. Electrochemistry

Electrochemical measurements were made using a CH instrument Model 630A Electrochemical Workstation. Cyclic voltammograms were obtained in a conventional and gastight three-electrode cell under Ar and at room temperature. The working electrode was a glassy carbon electrode (3 mm in diameter), the reference electrode a Ag/AgCl electrode (*ca.* -0.43 V vs. Fc/Fc^+), and the counter electrode a platinum wire. The supporting electrolyte is 0.1 M Bu₄NPF₆ in CH_3CN .

3. Results and discussion

3.1. Synthesis and characterization

$(\mu\text{-pdt})\text{Fe}_2(\text{CO})_6$ (**1**) was treated with $\text{Me}_3\text{NO} \cdot 2\text{H}_2\text{O}$ under the ice bath condition in CH_3CN in the atmosphere of N_2 [10], and then pyridine ligands (py, etpy or btpy) were added. Considerable yields of all the model complexes and their moderate stability in air as solid were ensured to research their properties.

The IR data of the CO bands for **A**, **B** and **C** show *ca.* 50 cm^{-1} shift to lower frequency compared to that of the all-carbonyl complex **1** (Table 2), and similar average ν_{CO} and the frequency range of the CO bands to those of different mono-subsituated complexes, *e.g.* $(\mu\text{-pdt})\text{Fe}_2(\text{CO})_5(\text{CN})$ (**3**) [10], $(\mu\text{-pdt})\text{Fe}_2(\text{CO})_5(\text{PPhMe}_2)$ (**4**) [15], $(\mu\text{-pdt})\text{Fe}_2(\text{CO})_5(\text{SEt}_2)$ (**5**) [19], which prove the considerable electron-donating capabilities of pyridine ligands. The ^1H NMR spectra of **A**, **B** and **C** each show typical signals for $\mu\text{-SCH}_2\text{CH}_2\text{CH}_2\text{S}$ at 2.15–2.16 and 1.85–1.86 ppm in spite of the introduction of pyridine groups. As shown in Table 3, it is interesting to observe that the chemical shifts for α - and β -H in pyridine groups are upfield-shifted as compared to those in non-coordinated pyridine complexes, indicating π -backdonation capability from diiron center to the pyridine ring.

3.2. X-ray crystallographic structures of complexes **A**, **B** and **C**

The structures of complexes **A**, **B** and **C** were determined by X-ray diffraction. Their molecular diagrams are depicted in Fig. 1, and the selected bond lengths and bond angles are given in Table 3. Complexes **A** and **B** crystallize in monoclinic $P2_1/n$ space group,

Table 1
Crystallographic data summary for complexes **A**, **B** and **C**.

	A	B	C
Empirical formula	$\text{Fe}_2\text{S}_2\text{C}_{13}\text{O}_5\text{H}_{11}\text{N}$	$\text{Fe}_2\text{S}_3\text{C}_{15}\text{O}_5\text{H}_{15}\text{N}$	$\text{Fe}_2\text{S}_3\text{C}_{17}\text{O}_5\text{H}_{19}\text{N}$
Formula weight	437.07	497.19	525.24
Space group	$P2(1)/n$	$P2(1)/n$	$P1$
<i>a</i> (Å)	8.200(3)	8.899(5)	9.342(6)
<i>b</i> (Å)	12.661(5)	22.291(10)	11.528(7)
<i>c</i> (Å)	16.094(7)	10.382(6)	11.564(7)
α (°)	90.00	90.00	66.769(17)
β (°)	90.717(5)	106.380(8)	79.15(3)
γ (°)	90.00	90.00	77.62(2)
<i>V</i> (Å ³)	1670.6(12)	1975.9(17)	1110.3(12)
<i>Z</i>	4	4	2
ρ_{calc} (g cm^{-3})	1.738	1.671	1.571
Absorption coefficient (mm^{-1})	2.007	1.810	1.615
Final <i>R</i> indices [<i>I</i> > 2 σ (<i>I</i>)]	$R_1 = 0.0359$ $\omega R_2 = 0.0929$	$R_1 = 0.0499$ $\omega R_2 = 0.0931$	$R_1 = 0.0591$ $\omega R_2 = 0.1295$
<i>R</i> indices (all data)	$R_1 = 0.0518$ $\omega R_2 = 0.1023$	$R_1 = 0.0913$ $\omega R_2 = 0.1098$	$R_1 = 0.1170$ $\omega R_2 = 0.1734$

Table 2
Listing of ν_{CO} infrared and electrochemical parameters for the model complexes **1–5**, **A**, **B** and **C**.

Complex	Ligand	ν_{CO} (KBr)/ cm^{-1}	Average value of $\nu_{\text{CO}}/\text{cm}^{-1}$	E_{pc1}/V vs. Ag/AgCl ($\text{Fe}^{\text{I}}\text{Fe}^{\text{I}}/\text{Fe}^{\text{I}}\text{Fe}^{\text{0}}$)	Reference
1	All-CO	2071, 2026, 1989, 1972	2015	−1.24	[29]
2	NH_2Pr	1980, 1943, 1907, 1892 ^a	1931 ^a	−1.36	[26]
3	CN^-	2029, 1974, 1955, 1941, 1917	1963	−1.73	[10]
4	PPhMe_2	2040, 1980, 1921	1980	−1.88	[15]
5	SEt_2	2045, 1976, 1960, 1919	1975	−1.29	[19]
A	py	2029, 1980, 1939, 1918	1967	−1.21	This work
B	etpy	2033, 1978, 1918	1976	−1.25	This work
C	btpy	2038, 1969, 1953, 1920	1970	−1.23	This work

^a ν_{CO} in THF.

Table 3
The chemical shifts for α - and β -H in pyridine groups.^a

	α -H	β -H
py	8.59	7.35
A	8.36	7.20
etpy	8.44	7.26
B	8.36	7.19
btpy	8.68	7.36
C	8.37	7.21

^a The chemical shift of acetonitrile is 1.96.

each with $Z = 4$. But complex **C** belongs to triclinic $P\bar{1}$ space group with $Z = 2$. Although the core structures of these molecules are all in the butterfly conformation, their sizes vary greatly (**A**, 1670.6(12) Å³; **B**, 1975.9(17) Å³; **C**, 1110.3(12) Å³).

As shown in Table 4, the displacement of one CO by pyridine ligands (py, etpy and btpy) has a slight influence on the Fe–Fe distance in **A**, **B** and **C** in comparison with that in **1** [29], as expected for mono-substituted diiron complexes. The angles of Fe(1)–Fe(2)–N(1) in complexes **A** and **B** are much smaller than that in complexes **C**; accordingly, the basal coordination mode of py and etpy on the Fe atoms in complexes **A** and **B** is different from the apical configuration of btpy in complexes **C** (Fig. 1). The bond lengths of the Fe(2)–N(1) in **A**, **B** and **C** lie in the narrow range 2.029(2)–2.030(5) Å, which are similar to that in **2** (2.033(5) Å) [26] and indicate weak Fe–N coordination.

Table 4
Selected bond lengths (Å) and angles (°) for complexes **A**, **B** and **C**.

Complex	A	B	C
Fe1–Fe2	2.5342(8)	2.5450(14)	2.506(2)
Fe1–S1	2.2600(12)	2.2654(14)	2.281(2)
Fe1–S2	2.2742(12)	2.2755(14)	2.2889(19)
Fe2–S1	2.2308(10)	2.2229(15)	2.285(2)
Fe2–S2	2.2475(10)	2.2519(15)	2.287(2)
Fe2–N1	2.029(2)	2.030(3)	2.030(5)
Fe1–Fe2–N1	103.26(8)	104.72(10)	146.24(14)
S1–Fe2–N1	158.90(7)	160.80(10)	101.92(14)
S2–Fe2–N1	86.08(7)	85.40(10)	99.39(14)
C4–Fe2–N1	100.68(13)	99.66(18)	100.7(2)
C5–Fe2–N1	92.87(12)	91.98(17)	100.5(2)

3.3. Cyclic voltammograms and electrochemical proton reduction

Complexes **A**, **B** and **C** were studied by cyclic voltammetry (CV) to evaluate the effects of the pyridine ligand on the redox properties of the model complexes. All the CV measurements were carried out in CH₃CN (with 0.1 M *n*-Bu₄NPF₆ as the electrolyte) and scanned in the cathodic direction (Fig. 2).

The electrochemistry of the complexes **A**, **B** and **C** all display two irreversible reduction peaks: the first reduction peaks appear at -1.21 to -1.25 V, and the second at -1.63 to -1.68 V. The first reductive potentials of the complexes **A**, **B** and **C** are 100–500 mV more anodic than those of **2–5** [10,15,19,26], and close to that of

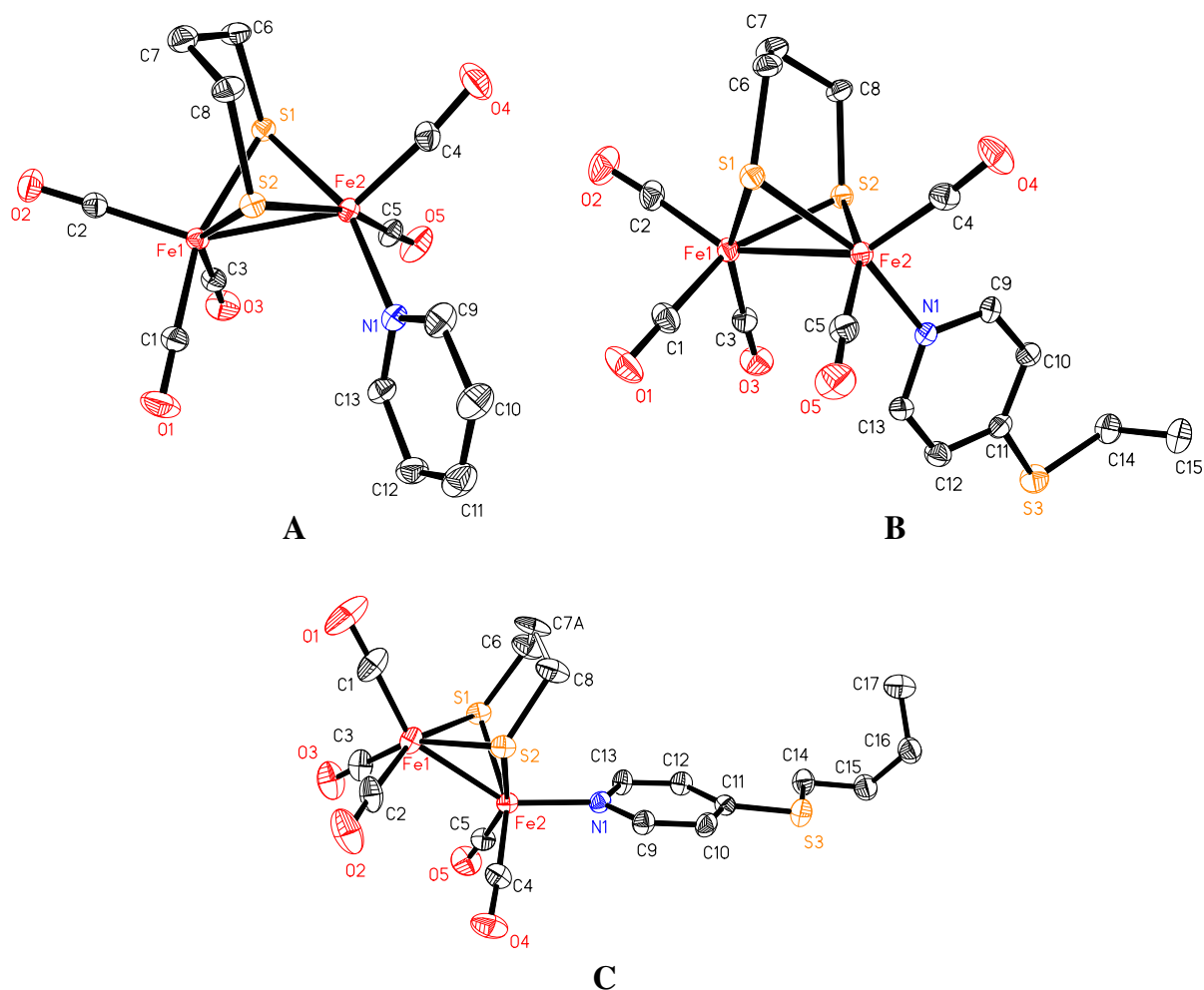


Fig. 1. Molecular structures of **A**, **B** and **C** with thermal ellipsoids at 30% probability. Hydrogen atoms are omitted for clarity.

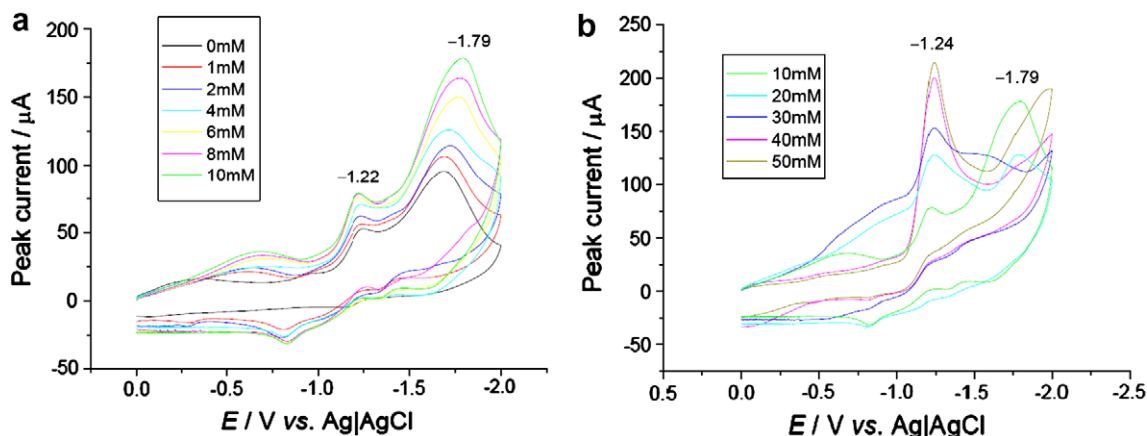


Fig. 2. Cyclic voltammogram of complex **B** (1.0 mM) with HOAc [(a) 0–10 mM and (b) 10–50 mM]. Supporting electrode is 0.1 M *n*-Bu₄NPF₆ in MeCN; working electrode: glassy carbon (0.0071 cm²); reference electrode: Ag|AgCl; scan rate = 0.1 V s⁻¹.

the all-CO complex **1** [29]. The electrochemical behavior conveys a message that, although the average electron density of the diiron centers of **A**, **B** and **C** are comparable to those of **2–5**, the π -orbitals of the pyridine ring can render the uneven electron density of the two iron atoms through an electron delocalisation. The strong π -accepting capability, also reported in substitutions of sulfoxides [20], suggests pyridine rings to be potential candidates to tune the electron properties of the diiron centers; this can be supported by another evidence that the carbene–pyridine disubstituted complex $(\mu\text{-pdt})\text{Fe}_2(\text{CO})_4(\text{NHC}_{\text{MePy}})$ displays similar reductive behaviors to those of the mono-substituents [6].

The electrochemical behavior of model **B** was analyzed in details in presence of HOAc (0–10 mM) as a source of protons (Fig. 2). The first reductive peak for **B** at ca. -1.24 V did not shift and the current height showed a minor growing, indicating that H⁺ did not incorporate to the model complex **B**. It was of particular interest that the second reduction peak for **B** shifted towards a more negative potential linearly with the addition of HOAc (0–10 mM), which electrochemical behavior features a proton relative process.

While HOAc was added continuously (10–50 mM), it is interesting that the first reductive peak increased distinctly while the second reductive peak reduced and disappeared at 30 mM of HOAc. Another measurement was made, in which 30 mM HOAc was added to the solution immediately. The first reductive peak at ca. -1.20 V grew dramatically, while the second one at -1.67 V disappeared at once. Under the effect of the excessive acid, complex **B** was proven to be reductive active at a rather low first reduction potential, while many other reported diiron model complexes were electrocatalytic inactive at the first reduction event in the presence of HOAc [32]. Functional and structural improvement on pyridine-N-ligands as good candidates to reduce the overpotentials of 2Fe₂S model complexes is in progress.

Abbreviations

etpy	4-(ethylthio)pyridine
btpy	4-(<i>n</i> -butylthio)pyridine
NH ₂ Pr	propylamine
NHC _{MePy}	1-methyl-3-(2-pyridyl)imidazol-2-ylidene
pdt	propanedithiolate
py	pyridine
SEt ₂	Ethyl thioether

Acknowledgements

The authors are grateful to the National Key Foundation of China (No. 20633020), the National Natural Science Foundation of Chi-

na (No. 20471061), the Science & Technology Innovation Foundation for Young Scholar of Fujian Province (No. 2007F3112) for financial support of this work.

Appendix A. Supplementary data

CCDC 670552, 670553 and 670554 contain the supplementary crystallographic data for **A**, **B** and **C**. These data can be obtained free of charge from The Cambridge Crystallographic Data Centre via www.ccdc.cam.ac.uk/data_request/cif. Supplementary data associated with this article can be found, in the online version, at doi:10.1016/j.jorganchem.2009.03.050.

References

- J.W. Peters, W.N. Lanzilotta, B.J. Lemon, L.C. Seefeldt, *Science* 282 (1998) 1853–1858.
- Y. Nicolet, C. Piras, P. Legrand, C.E. Hatchikian, *Structure* 7 (1997) 13–23.
- Y. Nicolet, A.L. de Lacey, X. Vernède, V.M. Fernandez, C.E. Hatchikian, J.C. Fontecilla-Camps, *J. Am. Chem. Soc.* 123 (2001) 1596–1601.
- J.F. Capon, S.E. Hassnaoui, F. Gloaguen, P. Schollhammer, J. Talarmin, *Organometallics* 24 (2005) 2020–2022.
- J.W. Tye, J. Lee, H.W. Wang, R. Mejia-Rodriguez, J.H. Reibenspies, M.B. Hall, M.Y. Darensbourg, *Inorg. Chem.* 44 (2005) 5550–5552.
- L.L. Duan, M. Wang, P. Li, Y. Na, N. Wang, L.C. Sun, *Dalton Trans.* (2007) 1277–1283.
- D. Morvan, J.F. Capon, F. Gloaguen, A. Le Goff, M. Marchivie, F. Michaud, P. Schollhammer, J. Talarmin, J.J. Yaoouanc, R. Pichon, N. Kervarec, *Organometallics* 26 (2007) 2042–2052.
- A.L. Cloiree, S.P. Best, S. Borg, S.C. Davies, D.J. Evans, D.L. Hughes, C.J. Pickett, *Chem. Commun.* (1999) 2285–2286.
- E.J. Lyon, I.P. Georgakaki, J.H. Reibenspies, M.Y. Darensbourg, *J. Am. Chem. Soc.* 123 (2001) 3268–3278.
- F. Gloaguen, J.D. Lawrence, M. Schmidt, S.R. Wilson, T.B. Rauchfuss, *J. Am. Chem. Soc.* 123 (2001) 12518–12527.
- J.L. Nehring, D.M. Heinekey, *Inorg. Chem.* 42 (2003) 4288–4292.
- C.A. Boyke, T.B. Rauchfuss, S.R. Wilson, M.M. Rohmer, M. Bénard, *J. Am. Chem. Soc.* 126 (2004) 15151–15160.
- X. Zhao, I.P. Georgakaki, M.L. Miller, J.C. Yarbrough, M.Y. Darensbourg, *J. Am. Chem. Soc.* 123 (2001) 9710–9711.
- X. Zhao, I.P. Georgakaki, M.L. Miller, R. Mejia-Rodriguez, C.Y. Chiang, M.Y. Darensbourg, *Inorg. Chem.* 41 (2002) 3917–3928.
- P. Li, M. Wang, C. He, G. Li, X. Liu, C. Chen, B. Åkermark, L. Sun, *Eur. J. Inorg. Chem.* (2005) 2506–2513.
- W. Dong, M. Wang, X. Liu, K. Jin, G. Li, F. Wang, L. Sun, *Chem. Commun.* (2006) 305–307.
- W. Dong, M. Wang, T. Liu, X. Liu, K. Jin, L. Sun, *J. Inorg. Biochem.* 101 (2007) 506–513.
- W. Gao, J. Ekström, J. Liu, C. Chen, L. Eriksson, L. Weng, B. Åkermark, L. Sun, *Inorg. Chem.* 46 (2007) 1981–1991.
- M.Q. Hu, C.B. Ma, X.F. Zhang, F. Chen, C.N. Chen, Q.T. Liu, *Chem. Lett.* 35 (2006) 840–841.
- M.Q. Hu, C.B. Ma, Y.T. Si, C.N. Chen, Q.T. Liu, *J. Inorg. Biochem.* 101 (2007) 1370–1375.
- T.B. Liu, M.Y. Darensbourg, *J. Am. Chem. Soc.* 129 (2007) 7008–7009.

- [22] C. Tard, X. Liu, S.K. Ibrahim, M. Rruschi, L.D. Gioia, S.C. Davies, X. Yang, L.S. Wang, G. Sawers, C.J. Pickett, *Nature* 433 (2005) 610–613.
- [23] J.L. Stanley, Z.M. Heiden, T.B. Rauchfuss, S.R. Wilson, L. De Gioia, G. Zampella, *Organometallics* 27 (2008) 119–125.
- [24] S. Ezzaher, J.F. Capon, F. Gloaguen, F.Y. Pétillon, P. Schollhammer, J. Talarmin, R. Pichon, N. Kervarec, *Inorg. Chem.* 46 (2007) 3426–3428.
- [25] N. Wang, M. Wang, T.B. Liu, P.L., T.T. Zhang, M.Y. Darensbourg, L.C. Sun, *Inorg. Chem.*, doi:10.1021/jc800525n.
- [26] L. Schwartz, J. Ekström, R. Lomoth, S. Ott, *Chem. Commun.* (2006) 4206–4208.
- [27] P.Y. Orain, J.F. Capon, N. Kervarec, F. Gloaguen, F.Y. Pétillon, R. Pichon, P. Schollhammer, J. Talarmina, *Dalton Trans.* (2007) 3754–3756.
- [28] A. Winter, L. Zsolnai, G. Huttner, *Z. Naturforsch.* 37b (1982) 1430–1436.
- [29] E.J. Lyon, I.P. Georgakaki, J.H. Reibenspies, M.Y. Darensbourg, *Angew. Chem., Int. Ed.* 38 (1999) 3178–3180.
- [30] G.M. Sheldrick, *SHELXS-97: Program for Crystal Structure Solution*, Institut für Anorganische Chemie der Universität, Göttingen, Germany, 1996.
- [31] G.M. Sheldrick, *SHELXL-97: Program for Crystal Structure Refinement*, Institut für Anorganische Chemie der Universität, Göttingen, Germany, 1997.
- [32] D.S. Chong, I.P. Georgakaki, R. Mejia-Rodriguez, J. Samabria-Chinchilla, M.P. Soriaga, M.Y. Darensbourg, *Dalton Trans.* (2003) 4158–4163.